

## Tomographic Assessment of Fusion Rate, Implant-Endplate Contact Area, Subsidence, and Alignment With Lumbar Personalized Interbody Implants at 1-Year Follow-Up

Christopher P. Ames, Justin S. Smith and Rodrigo J. Nicolau

*Int J Spine Surg* published online 27 August 2024  
<https://www.ijssurgery.com/content/early/2024/08/27/8640>

This information is current as of August 27, 2024.

---

**Email Alerts** Receive free email-alerts when new articles cite this article. Sign up at:  
<http://ijssurgery.com/alerts>

# Tomographic Assessment of Fusion Rate, Implant-Endplate Contact Area, Subsidence, and Alignment With Lumbar Personalized Interbody Implants at 1-Year Follow-Up

CHRISTOPHER P. AMES, MD<sup>1</sup>; JUSTIN S. SMITH, MD, PhD<sup>2</sup>; AND RODRIGO J. NICOLAU, MD<sup>3</sup>

<sup>1</sup>Department of Neurological Surgery, University of California, San Francisco, CA, USA; <sup>2</sup>Department of Neurosurgery, University of Virginia, Charlottesville, VA, USA; <sup>3</sup>Carlsmed, Carlsbad, CA, USA

## ABSTRACT

**Background:** Incongruity between irregularly shaped vertebral endplates and the uniform surfaces of stock interbody fusion cages has been identified as contributing to cage subsidence, pseudarthrosis, and unpredictable alignment. Advances in manufacturing techniques have driven the development of personalized interbody cages (PICs) that can match individual endplate morphology and provide the exact shape and size needed to fill the disc space and achieve the planned correction. This study used computed tomography (CT) imaging to evaluate the implant-endplate contact area, fusion, subsidence, and achievement of planned alignment correction in patients receiving PIC devices.

**Methods:** This retrospective study included patients treated for adult spinal deformity at a single site and implanted with PIC devices at L4 to L5 or L5 to S1 for segmental stabilization and alignment correction, who received 1-year postoperative CT images as part of their standard of care. An evaluation using 3-dimensional thin-section scans was conducted. Implant-endplate contact and signs of fusion were assessed in each CT slice across both endplates. The degree of subsidence as well as measures of segmental and global lumbar alignment were also assessed.

**Results:** Fifteen patients were included in the study, with a mean age of 68.2 years. Follow-up ranged between 9 and 14 months. Twenty-six total lumbar levels were implanted; 20 with PIC devices via the anterior lumbar interbody fusion approach, 2 with stock cages via the anterior lumbar interbody fusion approach, and 4 with PIC devices via the transforaminal lumbar interbody fusion approach. CT analysis of PIC-implanted levels found an overall implant-endplate contact area ratio of 93.9%, a subsidence rate of 4.5%, a fusion rate of 100%, and satisfactory segmental and global lumbar correction compared with the preoperative plan.

**Conclusions:** PIC implants can provide nearly complete contact with endplate surfaces regardless of the individual endplate morphology. Subsidence, fusion, and alignment assessments in this tomographic study illustrated results consistent with the benefits of a personalized interbody implant.

**Level of Evidence:** 4.

Lumbar Spine

Keywords: lumbar, interbody, fusion, personalized, contact, area, subsidence, alignment

## INTRODUCTION

Lumbar spine fusions are among the most common surgical procedures to address otherwise untreatable symptoms associated with instability and deformity involving different segments of the lower spine. The introduction of lumbar interbody fusion (LIF) cages and advances in interbody technologies and surgical approaches sought to enhance the outcomes of these procedures.<sup>1</sup> Among different efforts to advance LIF, cage materials having a stiffness closer to that of vertebral bone aimed to reduce rates of subsidence into the adjacent endplates and improve the rates of bony

fusion.<sup>2–4</sup> Cages with various lordotic angles were also developed in order to improve segmental and global spinal alignment.<sup>5,6</sup> In spite of these advances, subsidence rates for anterior lumbar interbody fusion (ALIF) and transforaminal lumbar interbody fusion (TLIF) procedures remain as high as 23.1% and 51.2%, respectively, in studies published within the past decade.<sup>7</sup> Rates of nonunion in the lumbosacral junction are reportedly up to 13% for L5 to S1 fusion, up to 20% for 2-level fusion,<sup>8,9</sup> and planned sagittal alignment, related to coronal and sagittal correction of individual segments, is achieved in only ~70%–75% of patients being treated for adult spinal deformity.<sup>10</sup> Akıntürk et al

performed a meta-analysis of 59 adult spinal deformity studies having a minimum follow-up of 1 year and identified an average rate of implant-related complications of 15.3%, including a 13.5% incidence of rod fracture.<sup>11</sup> Adogwa et al reported higher rates of rod fracture, noting that this complication is considered a proxy for pseudarthrosis.<sup>12</sup>

The diverse morphology of degenerated endplates has been recognized as having an influence on the success rate of LIF procedures. Irregular endplate morphology is a risk factor for both cage subsidence and migration, as it affects how well stock cages, with their preset shapes, sizes, and angles, interface with the unique anatomy of each patient's vertebral body and

endplate surface.<sup>13</sup> Increased overall contact between interbody cages and the adjacent endplates has been shown to improve postoperative disc height maintenance and angular correction.<sup>14</sup>

Advances in three-dimensional (3D) image acquisition and additive manufacturing technology have driven the development of interbody cages that better fit the specific level being treated by addressing the specific morphology.<sup>15</sup> With this approach, computed tomography (CT) scans of a patient's spine are reconstructed in 3D space, with the resulting image manipulated to meet the surgeon's planned segmental and global alignment goals. A 3D model of the resulting disc spaces and endplate surfaces intended for fusion is then used

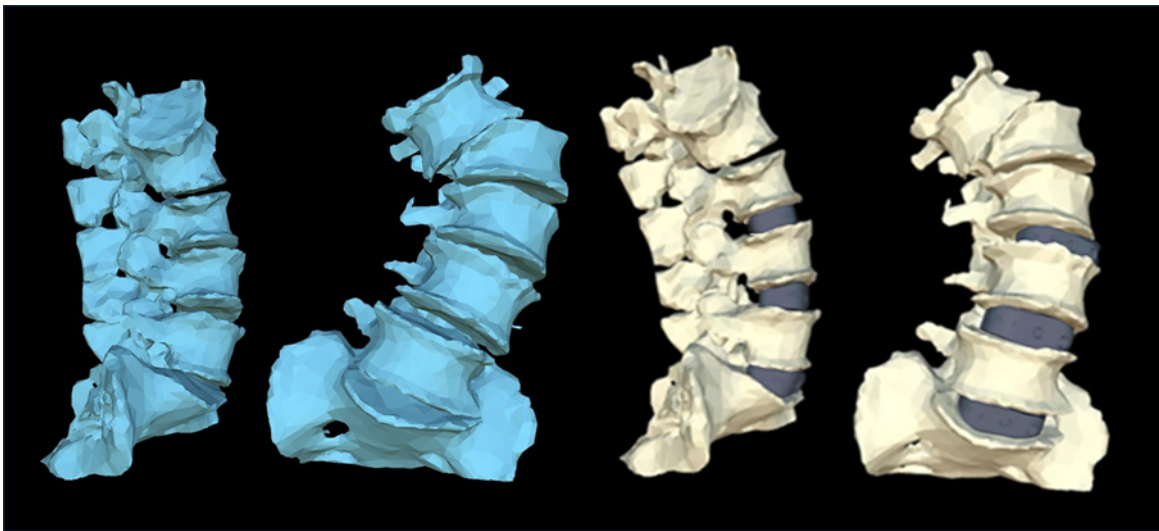


**Figure 1.** Sagittal and coronal views of 3-dimensional (3D) reconstruction of the preoperative condition (blue) and 3D model of planned correction (beige).

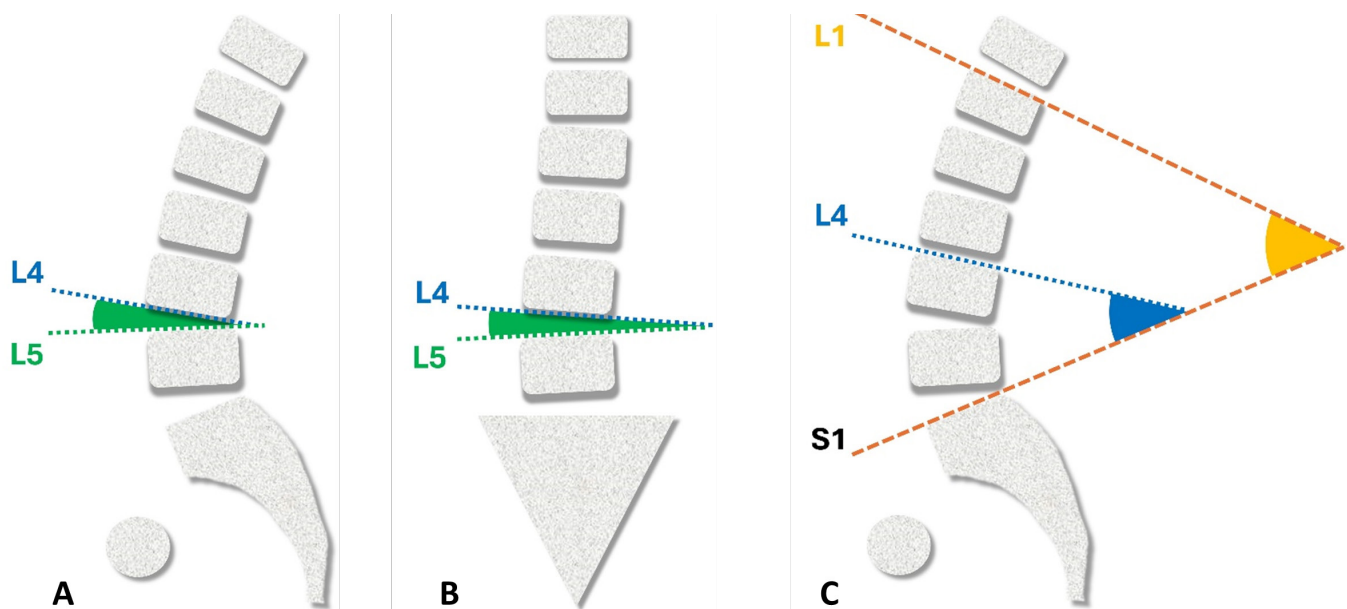


**Figure 2.** Sagittal and coronal L4 to L5 intervertebral angles (A and B); L1 to S1 lordosis and L4 to S1 angles (C).

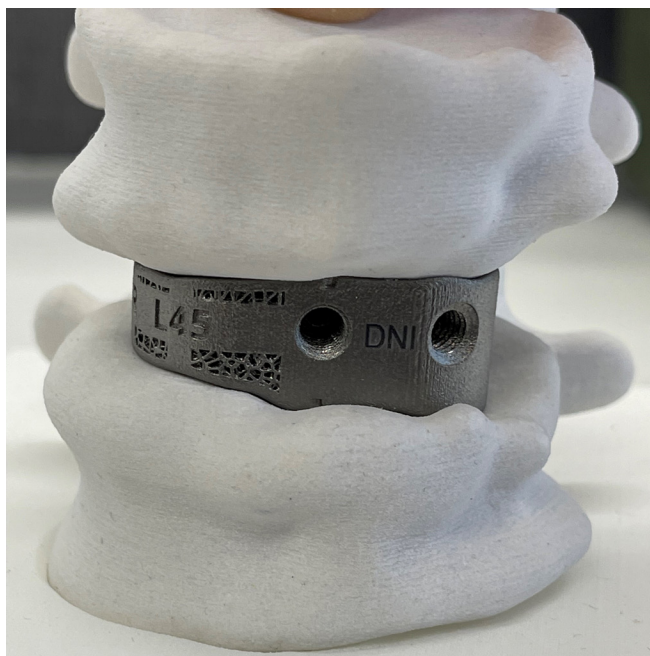


**Figure 3.** A personalized implant in a model illustrating coronal correction and added lordosis, along with added anterior/posterior height and contact surfaces designed to match the inferior and superior endplate shape.

to program the construction of personalized interbody cages (PICs) from a titanium alloy using additive manufacturing techniques (ie, 3D printing).<sup>15,16</sup> The objective of this tomographic study was to determine the effectiveness of PIC devices in providing improved contact with the endplates, as well as an assessment of fusion, subsidence, and achievement of segmental and global lumbar alignment goals.

## METHODS

Patients included in this retrospective evaluation underwent spinal fusion surgeries to address adult spinal deformity by 1 senior spine surgeon at a single institution. This study utilized secondary research consisting of deidentified data involving on-label use of a US Food and Drug Administration–cleared device and is therefore exempt from review by an institutional review board under Common Rule requirements.

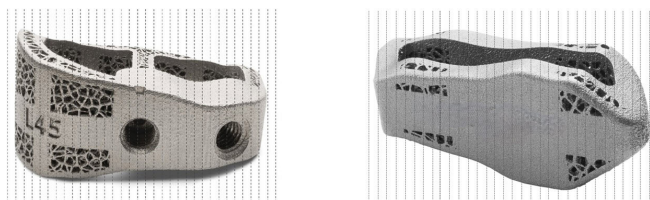


**Figure 4.** Illustration of coronal computed tomography slices for representative anterior lumbar interbody fusion and transforaminal lumbar interbody fusion personalized interbody cage implants.

**Table 1.** Bridwell fusion stage classification.

Fusion Grade	Description
I	Fused with remodeling and trabeculae present
II	Graft intact, not fully remodeled and incorporated, but no lucency present
III	Graft intact, potential lucency present at top and bottom of graft
IV	Fusion absent, with collapse/resorption of graft

PICs, ALIF or TLIF, were implanted as part of these surgeries at 1 or 2 levels (L5–S1 or L4–S1) for lumbar segmental stabilization and angular correction. Patients with at least 1 PIC implanted were included only if a spine tomographic study was performed as part of standard care approximately 1 year after the spinal fusion.

The personalized implants were manufactured for each patient by first creating a 3D model of planned correction based on the segmentation of the CT image of the affected spine (Figure 1). The 3D model incorporated the goals for intervertebral lordosis angle, intervertebral coronal angle, posterior disc height, L1 to S1 lordosis, and L4 to S1 angle as determined by the surgeon for each patient (Figure 2).

The geometry of each implant was determined based on the desired alignment of the vertebrae (using the virtual 3D model) as well as the specific morphology of the patient's inferior and superior endplates (Figure 3). The resulting implants were manufactured from a titanium alloy using additive manufacturing techniques.

3D thin-section (1 mm) CT spinal scans of each patient were performed at approximately 1-year follow-up with subsequent production of multiplanar reconstructions, including axial, coronal, and sagittal images. An independent spine surgeon evaluated all CT slices for the contact area of the implant to the endplate, cage subsidence, and degree of fused local bone inside cages. An evaluation of the alignment was also

**Table 2.** Operative characteristics.

Characteristic	Value
Patient	<i>N</i> = 15
Age, y, mean (SD)	68.2 (7.1)
Follow-up, mo, mean (range)	12.2 (9–14)
No. of levels instrumented, mean (SD)	10.4 (3.0)
Interbody implants	<i>N</i> = 26
Interbody implants per patient, mean (SD)	1.6 (0.6)
Level, <i>n</i> (%)	
L3–L4 (%)	2 (7.7%)
L4–L5 (%)	10 (38.4%)
L5–S1 (%)	14 (53.8%)
Procedure, No. of levels (%)	
ALIF PIC	20 (76.9%)
ALIF stock	2 (7.7%)
TLIF PIC	4 (15.4%)

Abbreviations: ALIF, anterior lumbar interbody fusion; PIC, personalized interbody cage; TLIF, transforaminal lumbar interbody fusion.



conducted to compare the intervertebral alignment achieved to each patient’s preoperative 3D personalized plan for the variables described above. All tomography analysis was conducted using DICOM viewer software (Radiant).

**Contact Area Ratio**

The parameters determined in CT scans were related to the analysis of every coronal and sagittal slice at the superior and inferior endplates (coronal CT slices shown in Figure 4). The area of the titanium surface of the implant in intimate contact with the endplate (ie, no discernable gaps) was compared with the total implant titanium surface available for contact to determine the implant-endplate contact area ratio. CT assessments of fusion included upper and lower segment endplates, trabecular bone contact, the presence of mature bony trabeculae bridging in interbody space, and signs of radiolucency around the implant and graft window.

**Subsidence**

Cage subsidence was evaluated at both the superior and inferior endplate on sagittal reconstruction CT imaging using the 4-grade assessment introduced by

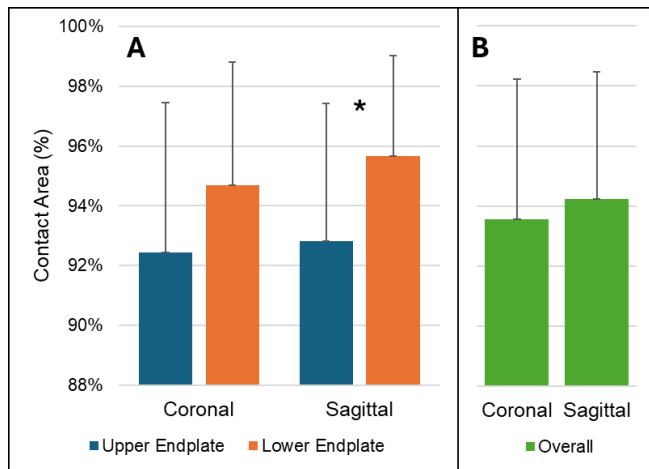


**Figure 5.** Ratio of available implant surface area in intimate contact with endplate (as a percentage). \*P < 0.05.

**Table 3.** Subsidence results.

Subsidence Grade	Degree of Subsidence	PIC ALIF (n = 20)	PIC TLIF (n = 4)	Stock ALIF (n = 2)
Grade 0	0%–24%	20 (100%)	3 (75%)	0
Grade I	25%–49%	0	1 (25%)	1 (50%)
Grade II	50%–74%	0	0	1 (50%)
Grade III	>75%	0	0	0

Abbreviations: ALIF, anterior lumbar interbody fusion; PIC, personalized interbody cage; TLIF, transforaminal lumbar interbody fusion.

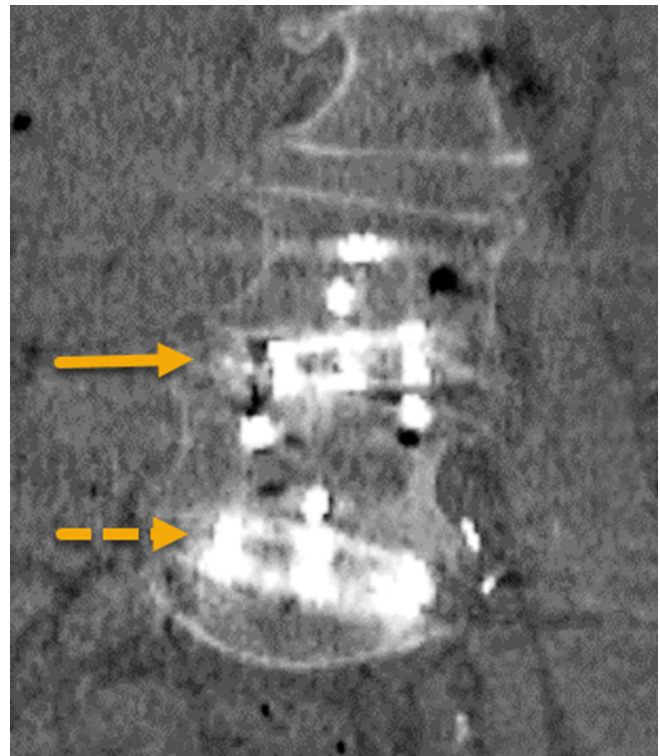


**Figure 6.** Two-level implantation showing moderate subsidence of stock cage into superior endplate at L4 to L5. The solid yellow arrow indicates the level treated with a stock implant. The dashed yellow arrow indicates the level treated with a personalized interbody cage.

Marchi et al<sup>14</sup> as grade 0: 0% to 24% loss of postoperative disc height; grade I: 25% to 49%; grade II: 50% to 74%; and grade III: 75% to 100%.

**Fusion**

The stages of fusion, as assessed at both the superior and inferior endplate by review of every CT slice of the implant-endplate interface, were quantified using the Bridwell classification (Table 1).<sup>17</sup>

**Angular Correction**

The alignment analysis of levels implanted with PIC devices compared measurements determined from the CT images for intervertebral lordosis, coronal angle, posterior disc height at the implanted PIC levels, L5 to

**Table 4.** Angular correction results.

Alignment Parameter	Offset Between Goal and Achieved, Mean (SD)
Intervertebral lordosis (PIC only)	1.3° (3.8°)
Intervertebral coronal angle (PIC only)	0.7° (1.5°)
Posterior disc height (PIC only)	-2.1 mm (2.0 mm)
L1–S1 lordosis (all patients)	3.1° (10°)
L4–S1 angle (all patients)	-0.9° (5.8°)

Abbreviation: PIC, personalized interbody cage.

S1 lordosis, and L4 to S1 angle to the correction goals set in the planning process, with results reported as deviations from the goals.

### Statistical Methods

Statistical analysis was performed using SPSS version 29.0.2.0. Descriptive statistics were reported as mean and SD or median and range for continuous variables depending on the data distribution and frequencies with percentages for categorical variables. For the comparison of contact areas, an arcsine transformation was applied to percentage data to improve normality, and comparisons were made using paired *t* tests. All tests were 2-tailed, with a significance level ( $\alpha$ ) of 0.05.

## RESULTS

Fifteen patients meeting the inclusion criteria and having CT's available at the time of this analysis were included in the study, having a mean age of 68.2 years (SD = 7.1). Personalized cages were placed at 24 levels (mean per patient = 1.6, SD = 0.6). In 2 patients, the senior surgeon chose to use 1 stock ALIF cage at the adjacent level. The majority of personalized cages were implanted via the ALIF approach (20; 83.3%), with the remainder implanted via the TLIF approach (4; 16.7%). The mean number of instrumented levels was 10.4 (SD = 3.0). Complete operative characteristics are shown in Table 2.

The assessment of contact between the implant and the endplates found an overall average of 93.9% of the available PIC surface area in contact with the adjacent endplates, with  $93.6\% \pm 4.7\%$  and  $94.3\% \pm 4.2\%$  contact when measured in coronal and sagittal views, respectively (Figure 5). The average contact ratio at lower endplates is higher in both coronal and sagittal views, although statistically significant differences are only observed in the sagittal view ( $P < 0.05$ ). The endplate-implant contact area for the 2 stock ALIF cages was also evaluated at the superior and inferior endplates, with an overall average of 81.9%. For the superior endplate, the average contact area was 94.6% in the coronal view and 95.6% in the sagittal view. For the inferior endplate, the average contact area was 67.5% in the coronal view and 70% in the sagittal view.

Grade I (moderate) subsidence was found in 1 level implanted with a PIC device via the TLIF approach with no subsidence seen in ALIF levels having a PIC implant (Table 3). Both stock implants were assessed as having subsided into the endplates, 1 with grade I

(Figure 6), and the other with grade II (high-grade). No rod fractures were observed at any level.

Complete fusion assessed as Bridwell Grade I on CT images was observed in 100% of the levels implanted with PIC implants at 1-year follow-up. For the 2 levels implanted with stock cages, both were assessed as grade II, that is, graft intact, but not fully remodeled and incorporated.

The results of the angular correction analysis are shown in Table 4. Only levels implanted with PIC devices were included in the analysis of intervertebral lordosis, intervertebral coronal angle, and posterior disc height because the intervertebral goals at stock cage levels were unknown. The measures of L1 to S1 lordosis and L4 to S1 angle included the patients implanted with stock cages.

## DISCUSSION

Degeneration of the intervertebral disc is characterized by numerous cellular and structural changes, including increased inflammatory activity, changes in collagen structure within the disc tissue, reduced permeability and vascular supply of vertebral endplate cartilage, and loss of hydrostatic pressure within the disc nucleus, all of which negatively impact both physiological and mechanical disc functions.<sup>18,19</sup> These changes can include increases in bony endplate porosity and decreases in trabecular bone thickness with increasing degeneration,<sup>20</sup> as well as increases in outward bulging of the annulus and overall loss of disc height leading to decreases in motion segment stiffness.<sup>21,22</sup>

Changes in lumbar endplate morphology are also related to disc degeneration. While endplates of healthy disc spaces are predominantly concave in the broadest sense,<sup>23-25</sup> the trend is to flatten and progress to an irregular morphology with increasing disc degeneration.<sup>26-28</sup> Variations in endplate morphology have been evaluated in relation to the endplate lesions commonly seen with the progression of disc degeneration, including calcification, fractures, erosion, and Schmorl's nodes.<sup>29,30</sup> The morphology of the degenerated endplate has significant implications for fusion procedures relying on interbody cages for stabilization and angular correction of the motion segment. A systematic review of failed interbody fusions by Yu et al identified an irregular disc space morphology as a risk factor for spacer subsidence into the endplate and spacer migration.<sup>13</sup>

## Contact Area Ratio

The advent of 3D printing technologies for intervertebral cages allows the design and production of cages shaped to fit the specific endplate morphology of an individual patient's disc space.<sup>15</sup> Computer modeling and biomechanical studies have both illustrated the benefits of PICs for interbody fusion. Chatham et al performed a finite element study based on the L4 to L5 level of a 70-year old man having flat endplates with uneven lateral heights, comparing a standard ALIF spacer having parallel, flat endplate contact surfaces to a custom spacer designed to conform to the curvature of the endplates. The authors found that the custom spacer reduced stresses at the endplate-spacer interface between 37% and 54% and reduced von Mises stresses in rods used for posterior stabilization by 28%–29% when compared with the standard spacer.<sup>31</sup> The results of a biomechanical study by Fernandes et al in cadaver spines found similar results in which a vertebral endplate could withstand up to 64% more force before subsidence occurred with a patient-specific implant than with standard cages.<sup>32,33</sup> This study also found that patient-specific cages increased the contact area between the cage and the endplate by up to 74% compared with commercially available cages, resulting in better utilization of the cage's total area, improved load sharing across the endplate, and significantly lower contact stress.<sup>32</sup>

While there are few CT-based clinical studies measuring the endplate-to-implant interface with stock interbody cages, the available literature is consistent with expectations based on bench studies, showing an increased risk of complications associated with reduced implant-endplate contact area ratios. These retrospective studies showed increased rates of non-union, cage subsidence, and pedicle screw loosening in patients having lower contact area ratios than in those with higher ratios.<sup>34,35</sup> Similarly, Lee et al reported a prospective controlled study of 78 PLIF levels in 54 patients. The ratio of the fused area of local bone inside the cages against the upper and lower vertebral endplates was measured by CT analysis at 1-year follow-up. The fusion area ranged from 46.4% to 52.2% of the available area, which was deemed insufficient for physiologic load transmission and the prevention of cage subsidence. Cage subsidence was found to be moderate in 41% of patients and substantial in 12% of patients.<sup>36</sup>

The overall average contact area ratio of 93.9% seen with the PIC implants in the current study is likely attributable to the personalized implant design closely

matching the patients' vertebral endplates to produce a lock and key fit. Any areas where the endplate did not make contact may be due to a minor area of osteointegration still being formed or image artifacts that did not allow for a precise visualization of that specific location. Both ALIF stock cages in this cohort developed subsidence at the superior endplate and had a comparatively low level of contact at the inferior endplate (67%–70%), leading to an overall average endplate-implant contact ratio of 81.9%.

## Subsidence

Cage subsidence primarily impacts restoration of disc height with its indirect decompression of the neural foramina resulting in increased stenosis and risk of symptom return, as well as increasing the risk of non-union and sagittal imbalance.<sup>14,37–39</sup> Subsidence in the current study was seen in only 1 of the 24 PIC levels (4.2%), implanted via the TLIF approach and assessed as moderate (grade II). In a systematic review of 20 articles reporting results on ALIF and TLIF procedures with stock cages, Parisien et al found subsidence rates for the ALIF approach of 6% to 23.1% and for the TLIF approach of 0.0% to 51.2%. The TLIF approach with posterior stabilization showed the highest median subsidence rates.<sup>7</sup>

## Fusion

The use of stock cages in ALIF and TLIF procedures for degenerative spine conditions has generally been reported with high mean fusion rates, in the range of 97.8% and 96.0%, for ALIF and TLIF, respectively.<sup>4</sup> However, in the treatment of adult spinal deformity, where rod fracture is viewed as a proxy for pseudarthrosis, a combined rod fracture rate of 19% was reported between patients receiving ALIF and TLIF interbody fusion, with 20.30% in the TLIF group and 16.92% in the ALIF group.<sup>12</sup> These data suggest that there remains a continued need to reduce nonunion rates, especially for providing stability of the lumbosacral junction for global sagittal balance in long fusions for deformity correction.<sup>40</sup> The 100% fusion rate for the 24 PIC implants in this study compares favorably against the results seen with stock cages and supports the concept of improved fusion rates resulting from increased implant-endplate contact and bone graft loading.

## Intervertebral Alignment Correction

A normal sagittal spinopelvic alignment contributes to maintaining a stable posture, and restoring sagittal



spinal balance has been shown to reduce pain, improve function, and reduce the risk of postoperative malalignment.<sup>41–43</sup> Proper alignment of the segments involved in lumbar fusion procedures has also been associated with improved patient quality of life.<sup>44</sup> Malalignment can result in inefficient energy use,<sup>14</sup> increased risk of adjacent level disease,<sup>45,46</sup> and recurrence of lumbar back and radicular pain.<sup>44</sup>

The need for proper lumbar alignment highlights the importance of achieving the planned intervertebral and lumbar lordosis. Considering the degree of disc space and segmental lordosis correction commonly sought in ALIF and TLIF procedures (up to 11° and 7°, respectively),<sup>5,47</sup> the mean offset of 1.3° found in levels implanted with PIC devices suggests that personalization of the interbody device may contribute to more precise intervertebral alignment.

### Limitations

The relatively small sample size of this study, combined with the limited available literature on similar CT analyses measuring endplate-to-implant contact with stock devices, limits the potential to make objective comparisons to other studies of stock devices. Another study with a larger cohort and a direct comparison to the use of stock implants performed by the same surgeon on patients with similar characteristics would enhance the analysis of postoperative alignment, fusion rate, and subsidence using PIC. The analysis of the implant-endplate interface was conducted based on CT analysis using a manual measurement methodology. Integrating a machine-learning computational tool would potentially enhance the analysis providing increased accuracy and precision. Finally, the observations are limited to ALIF and TLIF procedures.

### CONCLUSION

This 1-year follow-up CT analysis of PICs provides a unique opportunity to assess implant-to-endplate contact. Personalized interbody devices appear to offer a high level of endplate-to-implant contact at 1-year follow-up, which may contribute to improved interbody fusion rates, less subsidence, maintenance of alignment, and potentially decreased risk of implant-related complications.

### REFERENCES

1. Reisener MJ, Pumberger M, Shue J, Girardi FP, Hughes AP. Trends in lumbar spinal fusion—a literature review. *J Spine Surg.* 2020;6(4):752–761. doi:10.21037/jss-20-492

2. Verma R, Virk S, Qureshi S. Interbody fusions in the lumbar spine: a review. *HSS J.* 2020;16(2):162–167. doi:10.1007/s11420-019-09737-4

3. Formica M, Vallerga D, Zanirato A, et al. Fusion rate and influence of surgery-related factors in lumbar interbody arthrodesis for degenerative spine diseases: a meta-analysis and systematic review. *Musculoskelet Surg.* 2020;104(1):1–15. doi:10.1007/s12306-019-00634-x

4. Lenz M, Mohamud K, Bredow J, Oikonomidis S, Eysel P, Scheyerer MJ. Comparison of different approaches in lumbosacral spinal fusion surgery: a systematic review and meta-analysis. *Asian Spine J.* 2022;16(1):141–149. doi:10.31616/asj.2020.0405

5. Barrey C, Darnis A. Current strategies for the restoration of adequate lordosis during lumbar fusion. *World J Orthop.* 2015;6(1):117–126. doi:10.5312/wjo.v6.i1.117

6. Phan K, Mobbs RJ. Evolution of design of interbody cages for anterior lumbar interbody fusion. *Orthop Surg.* 2016;8(3):270–277. doi:10.1111/os.12259

7. Parisien A, Wai EK, ElSayed MSA, Frei H. Subsidence of spinal fusion cages: a systematic review. *Int J Spine Surg.* 2022;16(6):1103–1118. doi:10.14444/8363

8. Dinizo M, Passias P, Kebaish K, Errico TJ, Raman T. The approach to pseudarthrosis after adult spinal deformity surgery: is a multiple-rod construct necessary? *Global Spine J.* 2023;13(3):636–642. doi:10.1177/21925682211001880

9. Singh V, Oppermann M, Evaniew N, et al. L5-S1 pseudoarthrosis rate with ALIF versus TLIF in adult spinal deformity surgeries: a retrospective analysis of 100 patients. *World Neurosurg.* 2023;175:e1265–e1276. doi:10.1016/j.wneu.2023.04.113

10. Smith JS, Elias E, Sursal T, et al. How good are surgeons at achieving their preoperative goal sagittal alignment following adult deformity surgery? *Global Spine J.* 2023;23:219256822311613. doi:10.1177/21925682231161304

11. Akıntürk N, Zileli M, Yaman O. Complications of adult spinal deformity surgery: a literature review. *J Craniovertebr Junction Spine.* 2022;13(1):17–26. doi:10.4103/jcvjs.jcvjs\_159\_21

12. Adogwa O, Buchowski JM, Lenke LG, et al. Comparison of rod fracture rates in long spinal deformity constructs after transforaminal versus anterior lumbar interbody fusions: a single-institution analysis. *J Neurosurg Spine.* 2019;32(1):42–49. doi:10.3171/2019.7.SPINE19630

13. Yu Y, Robinson DL, Ackland DC, Yang Y, Lee PVS. Influence of the geometric and material properties of lumbar endplate on lumbar interbody fusion failure: a systematic review. *J Orthop Surg Res.* 2022;17(1):224. doi:10.1186/s13018-022-03091-8

14. Marchi L, Abdala N, Oliveira L, Amaral R, Coutinho E, Pimenta L. Radiographic and clinical evaluation of cage subsidence after stand-alone lateral interbody fusion. *J Neurosurg Spine.* 2013;19(1):110–118. doi:10.3171/2013.4.SPINE12319

15. Li S, Huan Y, Zhu B, et al. Research progress on the biological modifications of implant materials in 3D printed intervertebral fusion cages. *J Mater Sci Mater Med.* 2021;33(1):2. doi:10.1007/s10856-021-06609-4

16. Wilcox B, Mobbs RJ, Wu AM, Phan K. Systematic review of 3D printing in spinal surgery: the current state of play. *J Spine Surg.* 2017;3(3):433–443. doi:10.21037/jss.2017.09.01

17. Bridwell KH, Lenke LG, McEnery KW, Baldus C, Blanke K. Anterior fresh frozen structural allografts in the thoracic and lumbar spine. do they work if combined with posterior fusion and instrumentation in adult patients with kyphosis or anterior column



defects. *Spine*. 1976;20(12):1410–1418. doi:10.1097/00007632-199520120-00014

18. Velnar T, Gradisnik L. Endplate role in the degenerative disc disease: a brief review. *World J Clin Cases*. 2023;11(1):17–29. doi:10.12998/wjcc.v11.i1.17

19. Scarcia L, Pileggi M, Camilli A, et al. Degenerative disc disease of the spine: from anatomy to pathophysiology and radiological appearance, with morphological and functional considerations. *J Pers Med*. 2022;12(11):1810. doi:10.3390/jpm12111810

20. Rodriguez AG, Rodriguez-Soto AE, Burghardt AJ, Berven S, Majumdar S, Lotz JC. Morphology of the human vertebral endplate. *J Orthop Res*. 2012;30(2):280–287. doi:10.1002/jor.21513

21. Ashinsky BG, Gullbrand SE, Wang C, et al. Degeneration alters structure-function relationships at multiple length-scales and across interfaces in human intervertebral discs. *J Anat*. 2021;238(4):986–998. doi:10.1111/joa.13349

22. Zou J, Yang H, Miyazaki M, et al. Dynamic bulging of intervertebral discs in the degenerative lumbar spine. *Spine*. 2009;34(23):2545–2550. doi:10.1097/BRS.0b013e3181b32998

23. Lakshmanan P, Purushothaman B, Dvorak V, Schrott W, Thambiraj S, Boszczyk M. Sagittal endplate morphology of the lower lumbar spine. *Eur Spine J*. 2012;21 Suppl 2(Suppl 2):S160–4. doi:10.1007/s00586-012-2168-4

24. Wang Y, Battié MC, Videman T. A morphological study of lumbar vertebral endplates: radiographic, visual and digital measurements. *Eur Spine J*. 2012;21(11):2316–2323. doi:10.1007/s00586-012-2415-8

25. Singh T, Parr WCH, Choy WJ, et al. Three-dimensional morphometric analysis of lumbar vertebral end plate anatomy. *World Neurosurg*. 2020;135:e321–e332. doi:10.1016/j.wneu.2019.11.158

26. Pappou IP, Cammisa FP, Girardi FP. Correlation of end plate shape on MRI and disc degeneration in surgically treated patients with degenerative disc disease and herniated nucleus pulposus. *Spine J*. 2007;7(1):32–38. doi:10.1016/j.spinee.2006.02.029

27. Li Y, Lord E, Cohen Y, et al. Effects of sagittal endplate shape on lumbar segmental mobility as evaluated by kinetic magnetic resonance imaging. *Spine*. 2014;39(17):E1035–E1041. doi:10.1097/BRS.0000000000000419

28. Wang Y, Wang H, Lv F, Ma X, Xia X, Jiang J. Asymmetry between the superior and inferior endplates is a risk factor for lumbar disc degeneration. *J Orthop Res*. 2018;36(9):2469–2475. doi:10.1002/jor.23906

29. Wang Y, Videman T, Battié MC. Lumbar vertebral endplate lesions: prevalence, classification, and association with age. *Spine*. 1976;37(17):1432–1439. doi:10.1097/BRS.0b013e31824dd20a

30. Feng Z, Liu Y, Yang G, Battié MC, Wang Y. Lumbar vertebral endplate defects on magnetic resonance images: classification, distribution patterns, and associations with modic changes and disc degeneration. *Spine*. 1976;43(13):919–927. doi:10.1097/BRS.00000000000002450

31. Chatham LS, Patel VV, Yakacki CM, Dana Carpenter R. Interbody spacer material properties and design conformity for reducing subsidence during lumbar interbody fusion. *J Biomech Eng*. 2017;139(5):0510051–0510058. doi:10.1115/1.4036312

32. Fernandes RJR, Gee A, Kanawati AJ, et al. Biomechanical comparison of subsidence between patient-specific and non-patient-specific lumbar interbody fusion cages. *Global Spine J*. 2024;14(4):1155–1163. doi:10.1177/21925682221134913

33. Fernandes RJR, Gee A, Kanawati AJ, et al. Evaluation of the contact surface between vertebral endplate and 3D

printed patient-specific cage vs commercial cage. *Sci Rep*. 2022;12(1):12505. doi:10.1038/s41598-022-16895-9

34. Xie T, Pu L, Zhao L, et al. Influence of coronal-morphology of endplate and intervertebral space to cage subsidence and fusion following oblique lumbar interbody fusion. *BMC Musculoskelet Disord*. 2022;23(1):633. doi:10.1186/s12891-022-05584-3

35. Li JC, Xie TH, Zhang Z, Song ZT, Song YM, Zeng JC. The mismatch between bony endplates and grafted bone increases screw loosening risk for OLIF patients with ALSR fixation biomechanically. *Front Bioeng Biotechnol*. 2022;10:862951. doi:10.3389/fbioe.2022.862951

36. Lee JH, Jeon DW, Lee SJ, Chang BS, Lee CK. Fusion rates and subsidence of morselized local bone grafted in titanium cages in posterior lumbar interbody fusion using quantitative three-dimensional computed tomography scans. *Spine*. 2010;35(15):1460–1465. doi:10.1097/BRS.0b013e3181c4baf5

37. Frisch RF, Luna IY, Brooks DM, Joshua G, O'Brien JR. Clinical and radiographic analysis of expandable versus static lateral lumbar interbody fusion devices with two-year follow-up. *J Spine Surg*. 2018;4(1):62–71. doi:10.21037/jss.2018.03.16

38. Lewandrowski KU, Ransom NA, Yeung A. Subsidence induced recurrent radiculopathy after staged two-level standalone endoscopic lumbar interbody fusion with a threaded cylindrical cage: a case report. *J Spine Surg*. 2020;6(S1):S286–S293. doi:10.21037/jss.2019.09.25

39. Rao PJ, Phan K, Giang G, Maharaj MM, Phan S, Mobbs RJ. Subsidence following anterior lumbar interbody fusion (ALIF): a prospective study. *J Spine Surg*. 2017;3(2):168–175. doi:10.21037/jss.2017.05.03

40. Lee KY, Lee J-H, Kang K-C, et al. Strategy for obtaining solid fusion at L5-S1 in adult spinal deformity: risk factor analysis for nonunion at L5-S1. *J Neurosurg Spine*. 2020;33(3):323–331. doi:10.3171/2020.2.SPINE191181

41. Yuan JJ, Li G, Liu Y, Zhang Q, Ren ZS, Tian R. The association between sagittal spinopelvic alignment and persistent low back pain after posterior lumbar interbody fusion for treatment of mild L5-S1 spondylolisthesis: a retrospective study. *Int J Gen Med*. 2022;15:4807–4816. doi:10.2147/IJGM.S353797

42. Diebo BG, Balmaceno-Criss M, Lafage R, et al. Sagittal alignment in the degenerative lumbar spine: surgical planning. *J Bone Joint Surg Am*. 2024;106(5):445–457. doi:10.2106/JBJS.23.00672

43. He S, Zhang Y, Ji W, et al. Analysis of spinopelvic sagittal balance and persistent low back pain (PLBP) for degenerative spondylolisthesis (DS) following posterior lumbar interbody fusion (PLIF). *Pain Res Manag*. 2020;5971937. doi:10.1155/2020/5971937

44. Tchachoua Jiembou G, Nda HA, Konan ML. Evaluation of lordosis recovery after lumbar arthrodesis and its clinical impact. *Chin Neurosurg J*. 2023;9(1):18. doi:10.1186/s41016-023-00333-4

45. Kim JS, Phan K, Cheung ZB, et al. Surgical, radiographic, and patient-related risk factors for proximal junctional kyphosis: a meta-analysis. *Global Spine J*. 2019;9(1):32–40. doi:10.1177/2192568218761362

46. Buell TJ, Buchholz AK, Quinn JC, et al. Adjacent segment disease and proximal junctional kyphosis—part I: etiology and classification. *Contemp Neurosurg*. 2018;40(17):1–7. doi:10.1097/01.CNE.0000549709.01850.03

47. Watkins RG, Hanna R, Chang D, Watkins RG. Sagittal alignment after lumbar interbody fusion. *J Spinal Disord Tech*. 2014;27(5):253–256. doi:10.1097/BSD.0b013e31828a8447

**Funding:** This work was supported by funding from Carlsmed.

**Declaration of Conflicting Interests:**

Christopher P. Ames discloses that he is a clinical research investigator and receives consulting fees from Carlsmed. Justin S. Smith discloses that he is a shareholder and receives consulting fees from Carlsmed. Rodrigo J. Nicolau discloses that he is an employee of Carlsmed and receives or has received consulting fees, honoraria, support for attending meetings/travel, and stock/stock options from Carlsmed.

**Disclosures:** In addition to relationships listed in the Conflicts of Interest, Christopher P. Ames discloses that he has received grants or contracts from SRS; receives royalties or licenses from DePuy Synthes, K2M, Next Orthosurgical, Stryker, Biomet Zimmer Spine, Medcrea, and Nuvasive; receives consulting fees from DePuy Synthes, Medcrea, Agada Medical, Medtronic, and K2M; is the chair of the SRS Safety and Value Committee and serves on the ISSG Executive Committee; and has other financial/nonfinancial interests in Operative Neurosurgery and Neurospine (editorial boards), Global Spinal Analytics (director), and Titan Spine, ISSG, and DePuy Synthes (research). Justin Smith reports grants/contracts from SeaSpine

Orthofix, NREF, AOSpine, and DePuy Synthes; royalties/licenses from Highridge and Globus/NuVasive; consulting fees from Highridge, SeaSpine Orthofix, Medtronic, Cerapedics, and Globus/NuVasive; support for attending meetings/travel from AOSpine; serves on the SRS Board of Directors and ISSGF Executive Committee; and stock/stock options from Alphatec, Globus/NuVasive, and Carlsmed. Rodrigo J. Nicolau reports to be an employee of Carlsmed.

**IRB Approval:** This study utilized secondary research consisting of de-identified data for which consent is not required and was therefore exempt from institutional review board review under 45 CFR §46.104 (d)(4)(ii). No direct patient involvement occurred.

**Corresponding Author:** Christopher P. Ames, MDUCSF - Department of Neurological Surgery, 400 Parnassus Ave, A2300, San Francisco, CA 94143, USA; amesc@neurosurg.ucsf.edu

This manuscript is generously published free of charge by ISASS, the International Society for the Advancement of Spine Surgery. Copyright © 2024 ISASS. To see more or order reprints or permissions, see <http://ijssurgery.com>.